

# Migration in finely layered media

Kees Wapenaar and Wim van Geloven,  
Laboratory of Seismics and Acoustics,  
Delft University of Technology

August 12, 2005

## Introduction

It is well known that the relation between the angle-dependent reflectivity of an interface in a target zone and the amplitude-versus-offset effects (AVO) observed in the seismic data at the surface is complicated by many factors (Ostrander, 1984, GEOPHYSICS). Some of these factors are “reflection related” (such as thin bed tuning, reflector curvature), others “propagation related” (such as geometrical spreading, transmission and/or anelastic losses) or “acquisition related” (such as source/receiver directivity, geophone coupling). In this paper we address the reflection and propagation related *apparent* amplitude-versus-angle effects (AVA) of fine-layering and we discuss how to compensate for these effects in migration. The main steps in migration are downward extrapolation and imaging. An improved downward extrapolation scheme will compensate for the propagation related apparent AVA effects whereas the reflection related apparent AVA effects will be attacked with an improved imaging procedure.

## Propagation related AVA effects of fine-layering

The propagation through a package of thin layers is accompanied with wavelet *dispersion*. This dispersion is caused by internal multiple scattering and depends on the propagation angle. Figure 1 shows a 1-D acoustic medium consisting of 15000 layers with a thickness of 10 cm each. The statistics of the fine-layering are described by fractal Brownian motion (Walden and Hosken, 1985, GEOPH. PROSP.; Herrmann and Wapenaar, 1992, 62nd SEG meeting). The average velocity  $\bar{c}$  equals 2500 m/s. We modeled upgoing plane waves, propagating from the bottom to the top of the configuration. The ray parameter  $p$  ranges from 0.0 to  $0.8/\bar{c}$ , hence, the propagation angle ranges from 0 to 53 degrees. The lower frame in Figure 1 shows the modeling input at the bottom of the configuration and the upper frame shows the modeling output at the top of the configuration. Note that the propagation related apparent AVA effects are significant.

## • Conventional downward extrapolation

Downward extrapolation using the common matched filter approach yields the result shown in the upper frame of Figure 2. A comparison with the lower frame in Figure 1 (which can be seen as the ideal downward extrapolation output) clearly shows that the matched filter approach fails in finely layered media.

## • Improved downward extrapolation

We developed a modified matched filter that compensates for the propagation related apparent AVA effects. The correction term in this modified filter can be derived entirely from the multi-dimensional cross-correlation of the reflection measurements. The result is shown in the lower frame in Figure 2. Note that this result shows a very good amplitude recovery up to very high propagation angles (compare with the lower frame of Figure 1).

## Reflection related AVA effects of fine-layering

The reflection of a package of thin layers is accompanied with wavelet *interference*. Since, for a given frequency, the vertical wavelength  $\lambda_z$  varies with the angle of incidence (see Figure 3), the interference effects are also angle-dependent (see Figure 4).

## • Conventional imaging

Figure 5a shows a part of an angle-dependent reflectivity section, convolved with a seismic wavelet. It may be seen as the ideal output of imaging. Conventional imaging involves an integration of the downward extrapolated reflection data over all frequencies in the seismic band. The result is shown in Figure 5b. A comparison with Figure 5a clearly shows that the conventional approach fails in finely layered media.

## • Improved imaging

Due to the band-limitation of seismic data, the angle-dependent interference effects cannot be removed. However, we have developed a filter that *equalizes* these effects. This filter can be integrated in the imaging step in migration: for each angle the downward extrapolated data are integrated over a frequency band of constant  $\lambda_z$ . Figure 5c shows the result. It is a *band-limited* reflectivity section without reflection related apparent AVA (compare with Figure 5a). Figures 5d,e show that the improvements in the retrieved amplitudes are significant.

## Further developments

The examples shown in the previous sections have been obtained for 1-D media. We are currently extending the method for 2-D and 3-D media (see Figure 6). This involves the development of generalized primary propagators  $W_g^+$  and  $W_g^-$  that account for the propagation related apparent AVA effects in the 2-D or 3-D finely layered overburden. Furthermore, it involves the development of an improved imaging scheme that accounts for the reflection related apparent AVA effects in a locally tilted, finely layered target area, that to certain limits can be viewed as 1-D.

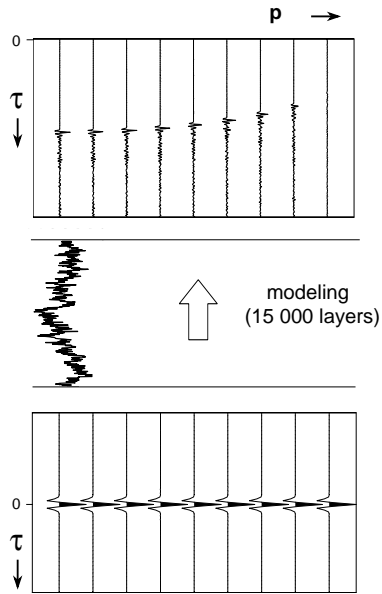


Figure 1: Upper frame: Plane wave transmission response.

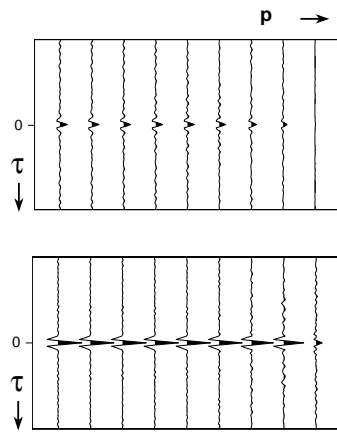


Figure 2: Downward extrapolation results using the matched filter and the modified matched filter, respectively.

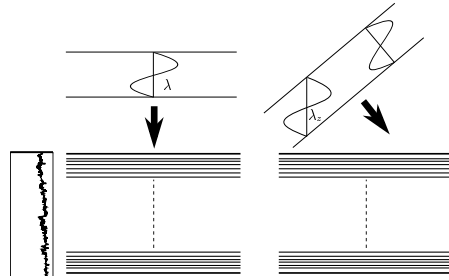


Figure 3: Different angles, same  $\omega \Rightarrow \lambda_z \neq \lambda$ .

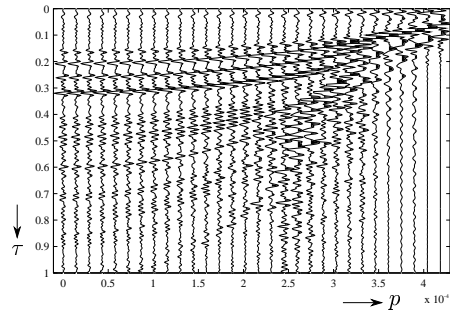


Figure 4: Plane wave reflection response.

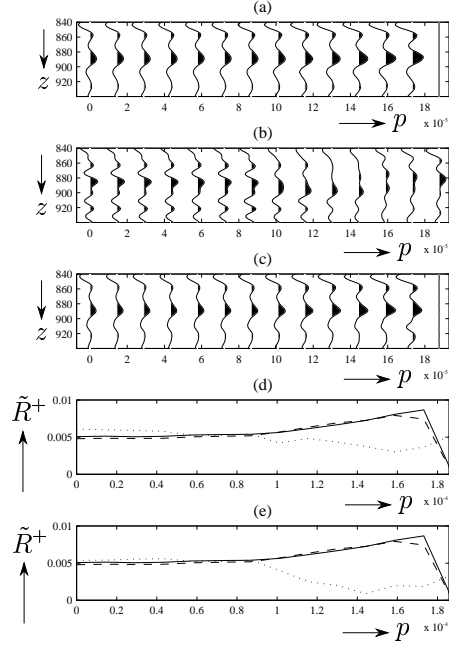


Figure 5: Reflectivity section around  $z = 890$  m. (a) Reference section. (b) Conventional imaging result. (c) Improved imaging result. (d) Picked amplitudes in a small band around  $z = 890$  m [solid: (a), dotted: (b), dashed: (c)]. (e) Picked amplitudes exactly at  $z = 890$  m.

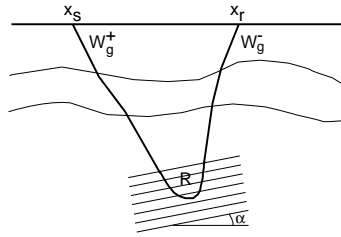


Figure 6: Multi-dimensional configuration.